ISSN 0965-545X, Polymer Science, Series A, 2016, Vol. 58, No. 3, pp. 386–398. © Pleiades Publishing, Ltd., 2016.
Original Russian Text © A.I. Prusskii, L.A. Aleshina, 2016, published in Vysokomolekulyarnye Soedineniya. Ser. A, 2016, Vol. 58, No. 3, pp. 268–281.

NATURAL POLYMERS

Computer Simulation of the Atomic Structure of Regenerated Cellulose

A. I. Prusskii* and L. A. Aleshina

Petrozavodsk State University, pr. Lenina 33, Petrozavodsk, 185000 Karelia, Russia
**e-mail: prusskiiandrey@gmail.com*

Received August 5, 2015; Revised Manuscript Received November 11, 2015

Abstract—The atomic structure of amorphous sulfate hardwood pulp obtained via regeneration in a dimethyl acetamide–LiCl solution is studied with the use of X-ray diffraction and computer simulation. When dimethyl acetamide appears within a cellulose chain, it becomes swollen. A chosen cluster has a complex structure and contains two cellulose chains II distorted by twisting and bending and two chains deformed by dimethyl acetamide molecules. A cluster with the formula unit $(C_6O_5H_{8.5}Li_{1.5}) \cdot (H_2O)_{2.8}$ is obtained after relaxation with the addition of water. The uncertainty-profile factor for the model and experimental curves of X-ray scattering intensity distribution $I(s)$ is 8%, and the distribution curve of s-weighted interference function $H(s)$ calculated for the model best fits the experimental curve.

DOI: 10.1134/S0965545X16030147

INTRODUCTION

Because of its composition, cellulose is insoluble or partially soluble in water and most commonly used organic solvents. Cellulose modification is necessary to obtain viscose fibers, films, membranes, and other cellulose-based products. One of the most successful ways of modification is the regeneration process [1] involving dissolution of cellulose I in a solvent followed by repeated precipitation during dilution with water.

At present, a mixture of dimethyl acetamide–lithium chloride (DMAA–LiCl) is more often used owing to its efficiency during dissolution of cellulose and other polysaccharides, especially those having high-molecular masses (M_w), such as cotton or bacterial cellulose [2].

As was shown in [3], the dissolution of wood cellulose in DMAA–LiCl gives rise to a homogeneous phase that determines the further use of the modified cellulose to obtain cellulose-based functional materials. However, the interaction of solvent molecules with cellulose at the molecular level is not yet completely understood.

For example, a plausible mechanism of cellulose dissolution in DMAA–LiCl was proposed on the basis of IR-spectral analysis [4]. It is assumed that protons of the hydroxyl groups of cellulose form strong hydrogen bonds with the Cl^- ion; as a result, intermolecular hydrogen bonds of cellulose are broken. Simultaneously, the Li^+–Cl^- ion pairs are separated and Li^+ cations are solvated on free DMAA molecules, thereby preserving the electrical balance. Then, cellulose chains are dispersed at the molecular level in a system of solvents to form a homogeneous solution.

The behavior of the solvent DMAA–LiCl in the course of cellulose dissolution was studied via the method of molecular-simulation [5]. In accordance with the authors of [5], DMAA poorly dissolves both LiCl and cellulose. As a result, DMAA molecules form stable bonds both with glucose residues and dissolved LiCl molecules. Unlike DMAA, water is a good solvent for LiCl, but not for cellulose; therefore, the dissolution of cellulose with the use of LiCl in the absence of water is impossible. The smallness of the Li^+ ion allows it to interact with a bridge oxygen; as a consequence, neighboring glucose residues converge. Therefore, the interaction between cellulose and Li^+ ions is much stronger than the interaction between cellulose and the large Cl^- ion. Hence, the higher the concentration of LiCl (the greater the amount of Li^+ ions), the better the dissolution of cellulose. In addition, the authors of [5] experimentally showed the replacement of DMAA with other molecules either worsens the solubility of cellulose or causes its complete insolubility [5]. Although DMAA dissolves a limited amount of LiCl, the interaction of lithium ions and glucose moieties is apparently so strong that the amounts of positive and negative ions in solution are enough for development of the process of glucose dissolution.

No data are available on the structural state of wood cellulose regenerated in the DMAA–LiCl system. X-Ray diffraction patterns [2] indicate that bac-

terial cellulose regenerated in the DMAA–LiCl system is amorphous.

In the study of amorphous materials, X-ray experiments provide one-dimensional information about their structures: radii and smearing of coordination spheres and coordination numbers. On the other hand, specific positions of atoms in space can be determined only via construction of computer models. In particular, it was shown that molecular simulation is a good tool to study the organization of cellulose chains in a material [6]. The amorphous cellulose considered in this study was generated and investigated with the use of the molecular-dynamics method; the simulated microstructures were mechanically stable.

The aim of this study was the investigation of the atomic structure of sulfate hardwood pulp regenerated in a DMAA–LiCl solution with the use of X-ray diffraction and computer simulation.

EXPERIMENTAL

X-Ray Diffraction Experiment and Data Treatment

In this study, the objects of research were samples of sulfate hardwood pulp in the initial powder state and after regeneration in a DMAA–LiCl solution (Laboratory of Chemistry of Plant Polymers, Institute of Chemistry, Komi Research Center, Ural Branch, Russian Academy of Sciences).

X-Ray diffraction patterns were registered on a DRON diffractometer in the automatic mode. In the initial state, the X-ray patterns of powder sulfate hardwood cellulose were obtained with the use of FeK_α radiation and CuK_α radiation in the reflection geometry. The specified character of mutual arrangement of cellobiose moieties in the unit cell of sulfate hardwood was refined, and its periods and the monoclinic angle were calculated with the use of a full-profile analysis performed via the Rietveld Method program of the PDWin 4.0 software package (NPP Burevestnik) [7].

In the full-profile analysis, functional (1) was reduced to the minimum

$$F = \sum_{i=1}^{N} w(i)[I_i^{\text{exp}} - I_i^{\text{theor}}]^2, \quad (1)$$

where I_i^{exp} and I_i^{theor} are the scattering intensities at the ith point of the X-ray diffraction pattern experimentally obtained for the studied sample and calculated for a crystal, respectively; $w(i)$ is the weight function, equal to $1/(dI_i^{\text{exp}})^2$; and N is the number of profile points.

The degree of discrepancy of experimental and theoretically calculated intensity distribution curves was evaluated from the value of uncertainty profile factor R_p:

$$R_p = \frac{\sum_{i=1}^{N} |I_i^{\text{exp}} - I_i^{\text{theor}}|}{\sum_{i=1}^{N} I_i^{\text{theor}}}. \quad (2)$$

For the crystalline phases of cellulose, theoretical X-ray diffraction patterns were determined from the atomic coordinates in a unit cell given in the Cambridge Structural Database (CSD).

The refinement procedure applied to cellulose objects was described in detail in [8, 9].

Cellulose samples regenerated in the DMAA–LiCl solution were studied with the use of FeK_α radiation and MoK_α radiation in the reflection and transmission geometries. The scattering image is isotropic.

Scattering-intensity-distribution curves $I(s)$ were normalized (via a change to electronic units), and s-weighted interference $H(s)$ and pair $D(r)$ functions were calculated with the use of the Warren–Finback method [9, 10]:

$$H(s) = s(I(s) - \sum\nolimits_j f_j^2(s))\exp(-\alpha^2 s^2)g^2(s), \quad (3)$$

$$D(r) = 2\pi^2 r\rho_e \sum\nolimits_j Z_j + \int_0^{s_{\max}} H(s)\sin(sr)ds, \quad (4)$$

where s is the length of the diffraction vector $\left(s = \frac{4\pi\sin\theta}{\lambda}\right)$; $\Sigma_j f_j^2(s)$ is the curve of independent atomic scattering with scattering amplitude $f_j(s)$ with summation over all the atoms of the formula unit of the compound; ρ_e is the average electron density of the material; α is the coefficient of attenuation factor $\exp(-\alpha^2 s^2)$, which is usually equal to 0.1; $g(s)$ is the peaking factor, equal to $g(s) = \frac{\sum_j f_j(s)}{\sum_j z_j}$; and Z_j is the atomic number of the jth element.

For the amorphous regenerated cellulose, coordination numbers N_{ij} were found from the $D(r)$ curves via the least squares method and SVD decomposition, while radii r_{ij} and smearing σ_{ij} of coordination spheres were estimated via the trial-and-error method [10]. The starting values of the radii and smearing of coordination spheres were the corresponding data calculated for the crystalline phase of cellulose II, because the phase transition of cellulose I into cellulose II happens during regeneration [11].

The reliability criterion of the obtained short-range-order characteristics (N_{ij}, r_{ij}, and σ_{ij}) was the value of q, which characterizes the degree of discrepancy of experimental curve $D(r)$ and curve $D_{\text{LSM}}(r)$.

The latter was calculated from the N_{ij} values obtained via the least squares method and the values of r_{ij} and σ_{ij} found via a trial-and-error search through the following formula:

$$D_{\mathrm{LSM}}(r) = \sum_{i=1}^{N}\sum_{j=1}^{M}\frac{N_{ij}}{r_{ij}}P_{ij}(r), \quad (5)$$

where summation over i and j is summation over the number of coordination spheres, N, set in calculations and the number of atoms in the formula unit, M, and $P_{ij}(r)$ is the pair function describing the electron-density distribution of one separate pair of atoms:

$$P_{ij}(r) = \int\limits_{i,j}^{N,M} f_i(s)f_j(s)e^{-(\alpha+\sigma_{ij})^2}\sin(sr_{ij})\sin(sr)dr. \quad (6)$$

The value of q was calculated [10] as mean-square deviation $\Delta D(r)$ at every point k of curve $D(r)$ calculated as a mean value over several (in this case, ten) curves, $D(r) = 0.1\sum_{m=1}^{10} D_m(r)$:

$$\Delta D(r_k) = \frac{\sum\limits_{m=1}^{10}(D_m(r_k) - D(r_k))^2}{k(k-1)},$$
$$q = \frac{\sum\limits_{k=l_{\min}}^{l_{\max}}\frac{|D(r_k) - D_{\mathrm{LSM}}(r_k)|}{D(r_k)}}{(l_{\max} - l_{\min}) + 1}\times 100\%. \quad (7)$$

The values of $l_{\min}$ and $l_{\max}$ limit the area of fitting of curves $D_{\mathrm{LSM}}(r)$ and $D(r)$ by the values of $r_{\min}$ and $r_{\max}$. That is, $r_{\min}$ corresponds to the beginning of the first maximum, while $r_{\max}$ is the radius of the last coordination sphere, for which the coordination number is calculated via the least squares method. In addition, the degree of coincidence of $D_{\mathrm{LSM}}(r)$ and $D(r)$ was evaluated visually from the plot.

Constructing the Computer Model

In [12], a single cellulose chain containing ten cellobiose moieties was used as the initial model for simulation of the atomic structure of mercerized cellulose modified with epichlorohydrin. It was found that the single chain insufficiently correctly describes the structure of the amorphous sample; therefore, in the present study, the initial model was a cluster obtained via a fivefold translation in the direction of the c axis of the unit cell of cellulose II, which contains two cellobiose moieties with the antiparallel orientation. The values of the unit-cell periods were a = 8.01 Å, b = 9.04 Å, and c = 10.36 Å, and the monoclinic angle was $\gamma = 117.1°$ [11].

Then, a series of cluster models was obtained via twisting of chains in the angular range 30°–360° with a step of 30°. The twisting technique was as follows: The initial fibril was divided into several fragments, and then every fragment was twisted so that the first and last fragments made a specified angle. Every twisted chain was bent by radii of 15, 20, 25, 30, 40, and 200 Å.

The optimization and relaxation of the distorted cluster models were performed with the use of the program HyperChem8. To minimize the cluster energy, the MM+ method, which is the basic method in HyperChem8, was chosen [13–15]. The MM+ force-field method is the improved version of MM2 developed for organic molecules [16–18]. This method allows for potential fields formed by all the atoms of the calculated system and makes it possible to flexibly modify calculation parameters, depending on a specific problem. As was verified in [19], the use of the MM+ group force fields is adequate for the construction of computer models of cellobiose [19]. As was noted in [20], MM+ is rarely used for the conformational analysis of hydrocarbons; nevertheless, application of this method yielded a number of good results.

The optimal structure of the entire system, when the full energy and its gradient are minimum, was calculated via the Polack–Ribière method, and relaxation was performed via the molecular-dynamics method.

Applicability of the constructed model to the description of the real structure of the material was checked with respect to the value of the uncertainty profile factor, which was calculated as

$$R_{\mathrm{pm}} = \frac{\sum\limits_{k}|I_{\exp}(s) - I_{\mathrm{mod}}(s)|_k}{\sum\limits_{i} I_{\mathrm{mod}\,k}(s)},$$

where $I_{\exp\,k}(s)$ and $I_{\mathrm{mod}\,k}(s)$ are the scattering-intensity distribution curves obtained in the experiment and calculated through the Debye method according to formula (6) [21]:

$$I(s)_{\mathrm{mod}\,k} = \frac{1}{N_{\mathrm{f}}}\left[\sum_{i=1}^{N} f_i^2 + 2\sum_{i}^{N-1}\sum_{j=i+1}^{N}\frac{1}{2}[f_i f_j^* + f_i^* f_j] \times\frac{\sin(sr_{ij})}{sr_{ij}}\exp\left(-\frac{1}{2}\sigma_{ij}^2 s^2\right)\right],$$

where f_i and f_j are the functions of atomic scattering of the ith and jth atoms, N is the number of atoms in the considered configuration, σ_{ij} is the dispersion of interatomic distances r_{ij} relative to the mean value, and N_{f} is the number of formula units in the configuration.

In addition, $H_{\mathrm{mod}\,k}(s)$ calculated from $I_{\mathrm{mod}\,k}(s)$ via formula (3) and the radial distribution functions of atoms, $W_{\mathrm{mod}}(r) = \dfrac{D_{\mathrm{mod}}(r)}{D_0(r)}$, were visually compared with experimental s-weighted interference functions

Table 1. Radii r_{ij} and smearing σ_{ij} of coordination spheres, coordination numbers N_{ij} of regenerated hardwood in comparison with the theoretically calculated values of sphere radii and coordination numbers for cellulose II

Kind of sphere	r_{ij}, Å	r_{ij} (cellulose II), Å	N_{ij}, at.	N_{ij} (cellulose II), at.	σ_{ij}, Å
C–O1	1.42	1.41	1.0	1.1	0.20
C–C1	1.55	1.54	1.5	1.6	0.05
C–O2	2.40	2.41	3.1	3.9	0.18
O–O1	2.86	2.86	4.6	4.2	0.15
O–O2	3.28	3.29	6.1	0.9	0.20
C–O3	3.63	3.66	3.3	4.7	0.14
C–C2	3.79	3.85	1.4	1.0	0.10
C–O4	3.96	3.96	4.7	1.9	0.15
$\Delta r_{ij} = \pm 0.01$ Å; $\Delta N_{ij} = \pm 0.1$ at.					

$H(s)$. The distribution curves of pair functions for models, $D_{mod}(r)$, were calculated from $H_{mod}(s)$ via formula (4).

The need to use $W(r)$ instead of $D(r)$ during comparison of the results of the experiment with the calculation data for the clusters is related to the fact that experimental curve $D(r)$ oscillates around the straight line $D_0(r) = 2\pi^2\rho_e\sum_j Z_j$ (Fig. 1a), whose slope is determined by the constant value of the mean electron density. Curve $D_{mod}(r)$ calculated for the model oscillates around the parabola (Fig. 1b) owing to the small dimensions of the model cluster [10]. The shape of curve $W(r)$ does not depend on the character of the mean-electron-density distribution of the model.

RESULTS OF X-RAY DIFFRACTION EXPERIMENTS

Figure 2 demonstrates the scattering-intensity-distribution curves for the initial and regenerated sulfate hardwood that were obtained in the reflection geometry with the use of FeK_α radiation. The positions of reflections in the X-ray diffraction patterns of the powder sulfate hardwood sample correspond to those of cellulose βI (the hatched diagram in Fig. 2a).

Both parallel and antiparallel arrangements of cellobiose moieties are possible in the unit cell of cellulose βI obtained from different kinds of wood and other types of native sources. In addition, the values of the unit-cell periods depend on the raw material and the route of synthesis [21].

With the use of the full-profile analysis, it was found that the initial sample of powder hardwood cellulose examined in this study has the monoclinic symmetry and the antiparallel mutual arrangement of molecules. The values of unit-cell periods are a = 7.98(5) Å, b = 8.03(2) Å, and c = 10.35(1) Å, and the monoclinc angle is $\gamma = 95.7(1)^\circ$. The uncertainty factor is $R_p = 5.33\%$ [22].

As is seen in Fig. 2b, the regeneration of sulfate hardwood cellulose in the DMAA–Li solution causes its amorphization because the X-ray scattering pattern obtained for the regenerated cellulose is diffuse.

The structure of amorphous cellulose was studied with the use of MoK_α radiation in the transmission mode.

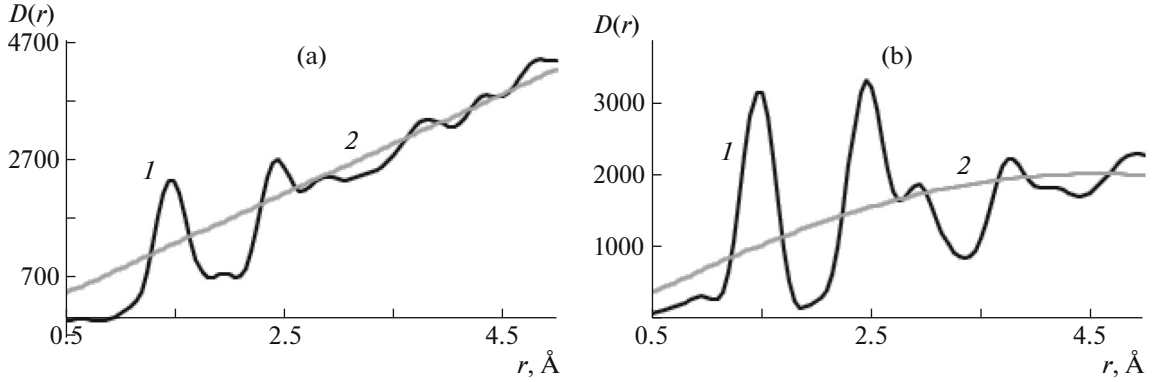

Fig. 1. Distribution curves of pair functions (*1*) $D(r)$ and (*2*) $D_0(r)$ calculated (a) from the experiment and (b) for the model of a confined volume.

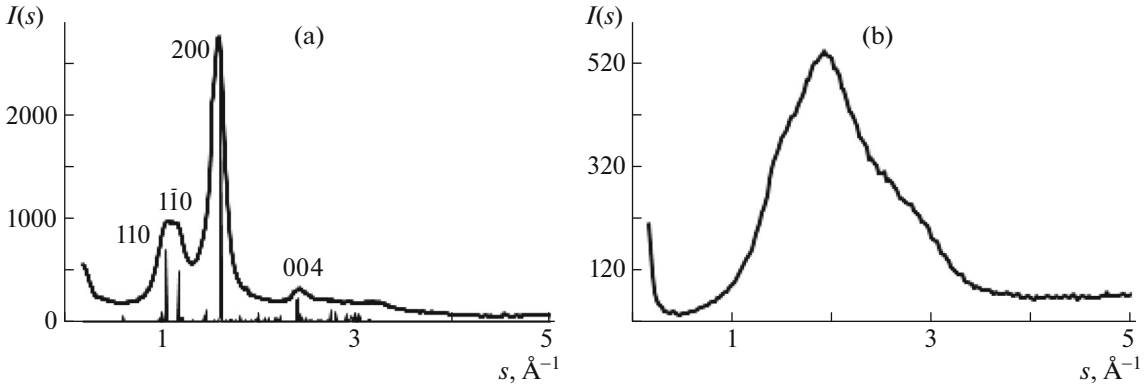

Fig. 2. Distribution curves of scattering intensity (eu) of sulfate hardwood cellulose: (a) powder cellulose in comparison with the hatched diagram of cellulose βI (the indices of main reflections are shown) and (b) regenerated cellulose.

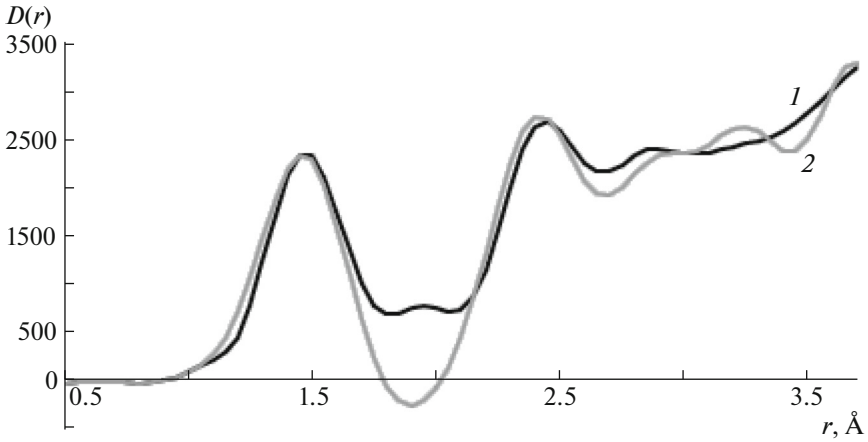

Fig. 3. Distribution curves of pair functions of regenerated hardwood: (*1*) the experimental $D(r)$ curve and (*2*) the calculated $D_{LSM}(r)$ curve.

The values of radii r_{ij}, smearing σ_{ij} of coordination spheres, and coordination numbers N_{ij} calculated on the basis of experimental curves $D(r)$ are summarized in Table 1.

Figure 3 presents the experimental $D(r)$ curves and the $D_{LSM}(r)$ curves calculated from the values of r_{ij}, N_{ij}, and σ_{ij} (Table 1) through formula (5) with allowance for (6). The degree of discrepancy of the presented curves is $q = 21\%$.

It is evident that the main difference between the calculated $D_{LSM}(r)$ and experimental $D(r)$ curves is observed in the vicinity of $r_{ij} \sim 1.9$ Å. Theoretical calculations show that the structure of the known modifications of cellulose does not contain pairs of atoms with interatomic distances close to 1.9 Å.

Moreover, at a sphere radii of $r_{ij} > 2.4$ Å, the values of coordination numbers do not coincide with the data calculated for the model of cellulose II. The cause of this discrepancy may be either a change in the relative orientation and lengths of cellulose chains in the amorphous state or a change in the chemical composition during the reaction with DMAA–LiCl. The molecular-dynamics method was applied to solve the problem.

Construction of Atomic Models via the Molecular-Dynamics Method

For the sake of comparison, Fig. 4 presents interference functions $H(s)$ calculated from the experimental data for the studied sample and the initial cluster model.

Distribution curves $H(s)$ for the studied sample and the theoretical cluster model of cellulose II are qualitatively similar, but for the theoretical curve, oscillations are narrower and, consequently, more intense in height. The value of R_{pm} is 0.28. The sharpness of oscillations may be reduced through the introduction of distortions in the initial cluster model [8, 21].

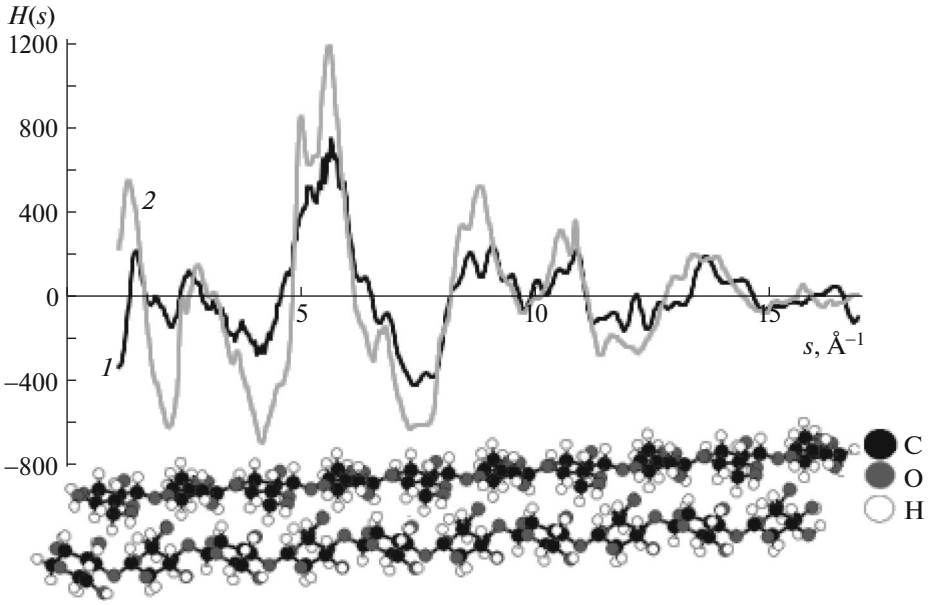

Fig. 4. Interference scattering functions $H(s)$: (*1*) the experimental curve for the samples of regenerated cellulose and (*2*) the calculated curve for the cluster model shown in the figure.

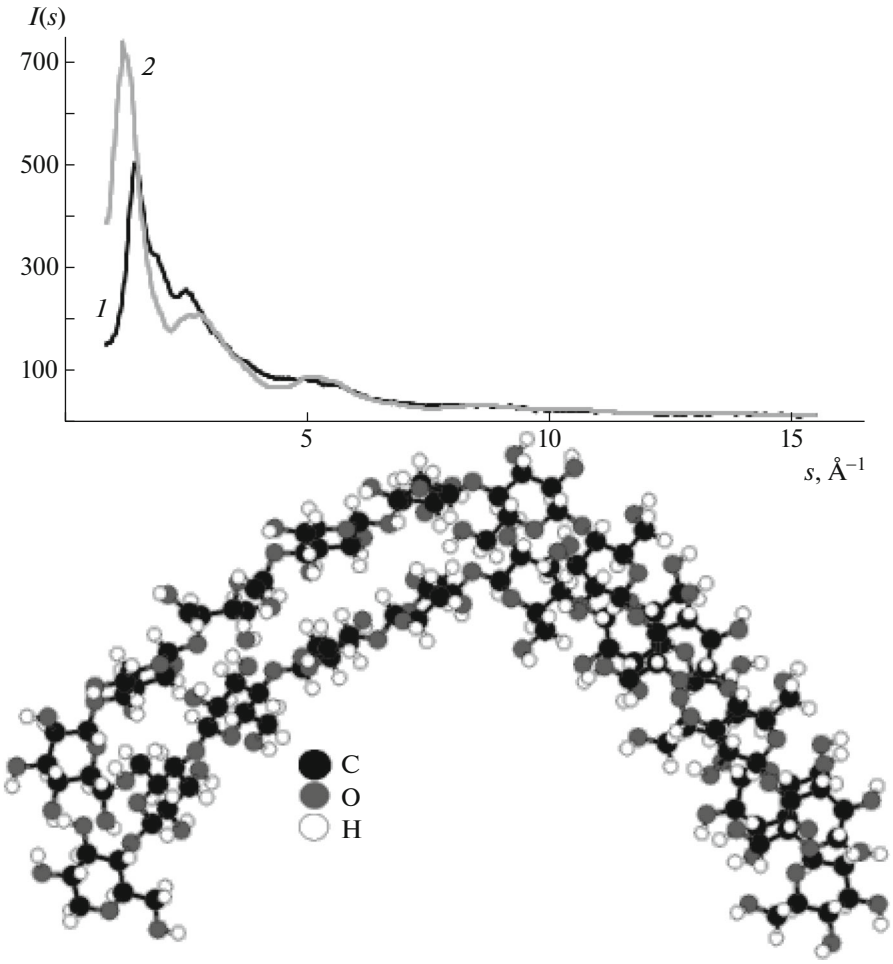

Fig. 5. Distribution curves $I(s)$: (*1*) the experimental curve for the samples of regenerated cellulose and (*2*) the calculated curve for the cluster model shown in the figure.

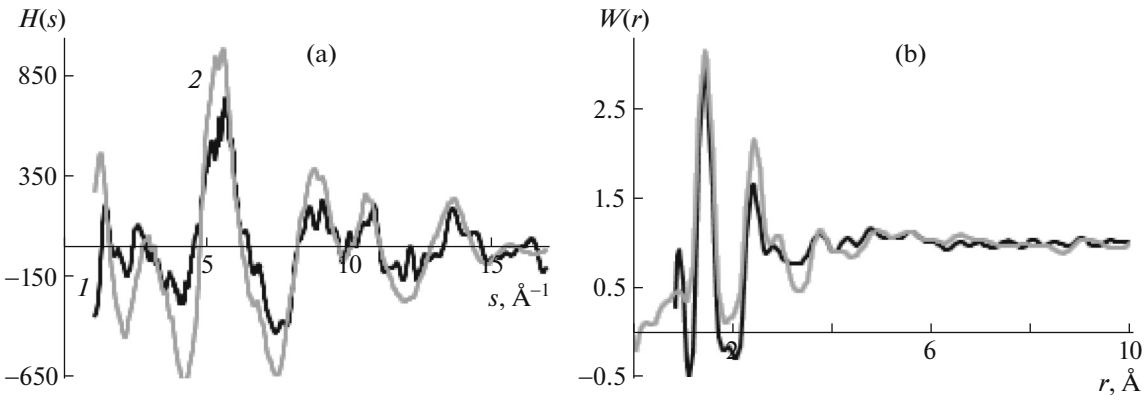

Fig. 6. (a) Distribution curves of interference functions $H(s)$ and (b) radial distribution functions of atoms, $W(r)$, for (*1*) the samples of regenerated cellulose in comparison with the corresponding curves (*2*) for the cluster model of cellulose II presented in Fig. 5.

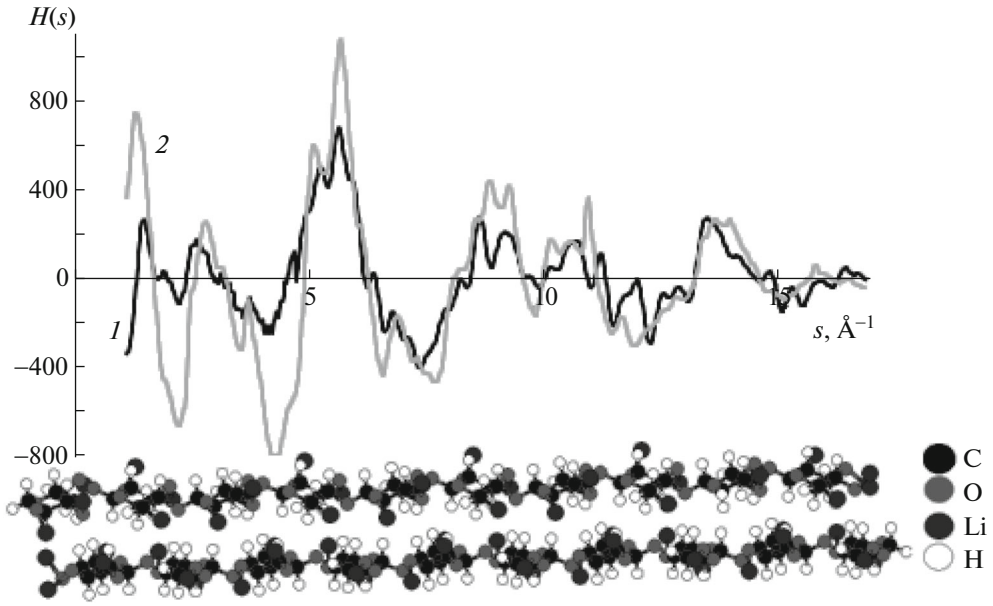

Fig. 7. Interference scattering functions $H(s)$: (*1*) the experimental curve for the samples of regenerated cellulose and (*2*) the calculated curve for the cluster model presented in the figure.

In [23], the structure of cellulose microfibrils obtained from green algae was studied with the use of atomic force microscopy. The studied sample was found to have regions where the observed fibrils are twisted. Generally, such regions are seen at a 700-nm interval along the microfibril, and, in all cases, they are twisted clockwise. Therefore, the fibers of cellulose model were deformed in this study.

The smallest value of R_{pm} (0.25) was found for the cluster twisted by 120° and bent to a radius of 15 Å (Fig. 5). The upper part of the figure additionally shows distribution curve $I(s)$ for such a twisted cluster. The corresponding $H(s)$ and $W(r)$ curves are presented in Fig. 6.

For curves $W(r)$ (Fig. 6b) calculated via the model and from the experiment, there is agreement between the position and intensity of the main maximum and the positions of the three next peaks. The coincidence of curves $H(s)$ (Fig. 6a) with the experimental results is still unsatisfactory. This circumstance means that, beyond the glucose moiety, the distribution of atoms in the cluster does not correspond to the real structure of the sample.

The process of regeneration of bacterial and native celluloses was studied in a DMAA–LiCl mixture [2]. On the basis of the experimental results, it was supposed that lithium ions can replace hydrogen atoms in OH groups. On the basis of this assumption, models

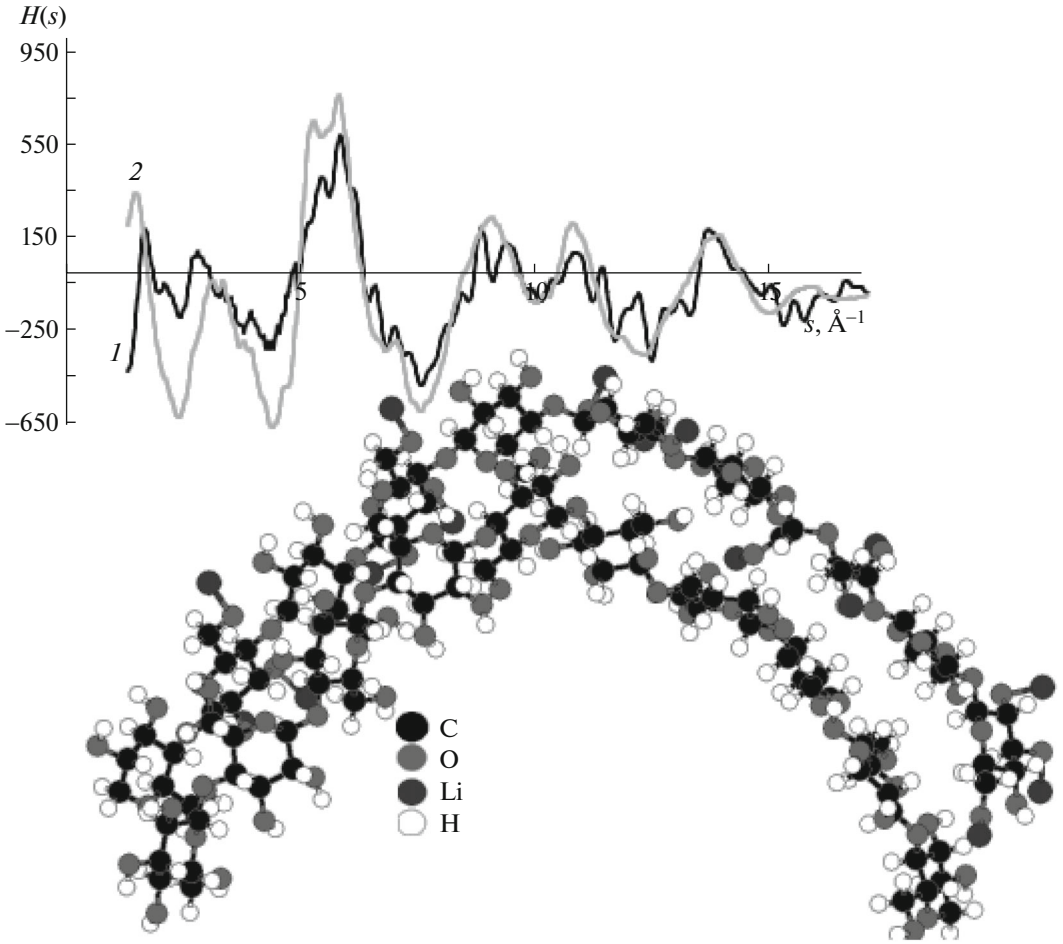

Fig. 8. Interference scattering functions $H(s)$: (*1*) the experimental curve for the samples of regenerated cellulose and (*2*) the calculated curve for the cluster model presented in the figure.

with different concentrations of Li ions were constructed. Among all the considered models, the cluster containing four Li ions per cellulose formula unit yielded scattering images closest to the experimental ones (Fig. 7).

For the curves calculated via the model, the intensities of oscillations increase. This fact may be explained not only by the replacement of hydrogen with lithium but also by the undeformed state of chains. The R_{pm} value is 0.28.

Then, the cluster (Fig. 7) was deformed, and the lowest value of R_{pm} was found for the cluster model twisted by 120° and bent by 15 Å: 0.18.

In Fig. 8, like in the previous case, the experimental $H(s)$ curves and the $H(s)$ curves calculated via the cluster model are similar; however, they have a number of distinctions. In particular, the maxima on curve $H(s)$ starting from 6 $Å^{-1}$ come nearer to the corresponding values observed on the experimental curve, but the discrepancy of the curves in the range of s values up to 5 $Å^{-1}$ is high.

On the basis of conditions of the regeneration process, it was suggested to adjust twelve molecules of DMAA (C_4H_9NO) in the cluster model with five translations of cellulose II. The DMAA molecule constructed with the use of the program HyperChem 8.0 is shown.

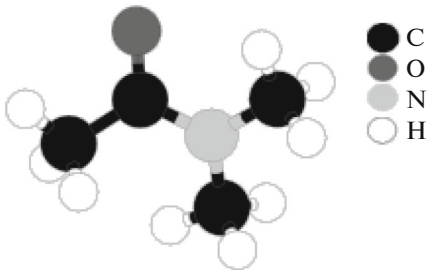

Figure 9 presents the undistorted cluster with five translations of cellulose II containing twelve DMAA molecules (C_4H_9NO) together with the corresponding distribution curves of interference functions $H(s)$. The value of R_{pm} is 0.32.

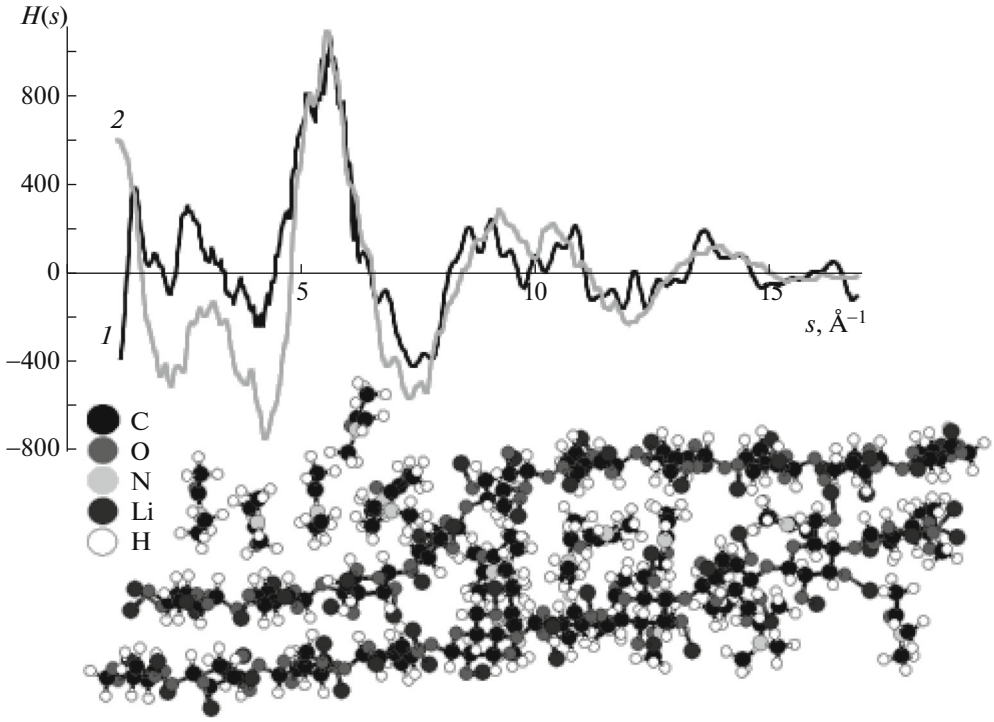

Fig. 9. Interference scattering functions $H(s)$: (*1*) the experimental curve for the samples of regenerated cellulose and (*2*) the calculated curve for the cluster model presented in the figure.

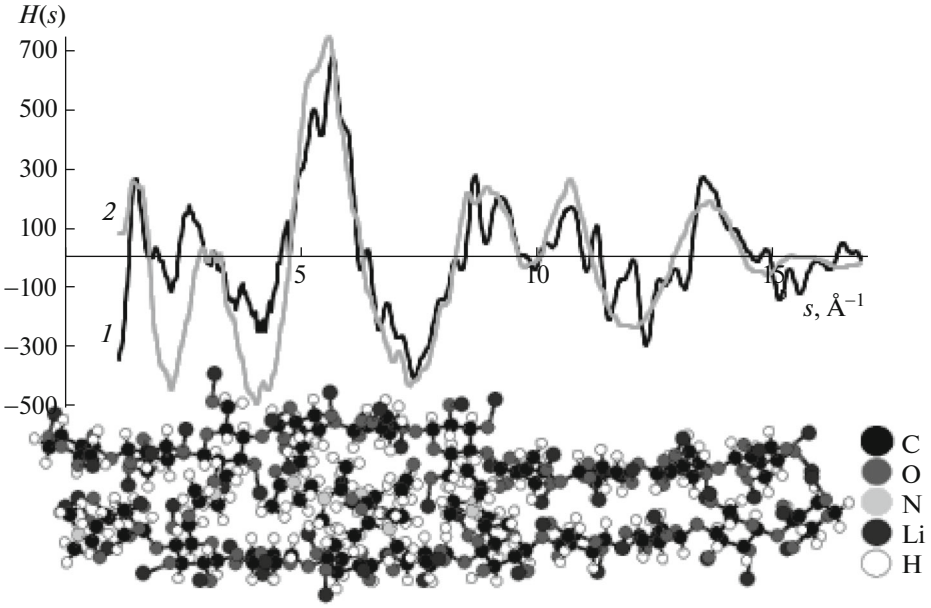

Fig. 10. Interference scattering functions $H(s)$: (*1*) the experimental curve for the samples of regenerated cellulose and (*2*) the calculated curve for the cluster model presented in the figure.

Then, cluster (Fig. 9) was deformed and the cluster model that is consistent with the experiment at $s > 5$ Å^{-1} was obtained at a twisting angle of 120° and a bending radius of 200 Å (Fig. 10). Nevertheless, for this cluster model, the value of R_{pm} was 0.27. In Fig. 10, the corresponding calculation data for the cluster model of cellulose are compared with the experimental data. It is evident that the addition of

DMAA molecules to the system causes a shift in the maxima on curve $H(s)$ at values of s from 2 to 5 Å^{-1}; this result may be explained by swelling of the cluster during incorporation of DMAA molecules into it.

Thus, after deformation of cellulose chains, the distribution curves of intensities and $H(s)$ calculated via the cluster model deviate from the experimental data in the range of s values both upward (Figs. 6, 7) and downward (Fig. 9). Better agreement of the experimental and calculated $H(s)$ curves was found at small radii of the circle around which the axis of the cellulose chains is bent.

On the basis of the above results, the next cluster was built. The unit cell of cellulose II was translated 5 times along axis c. The resulting cluster model was twisted by 120° and bent by 10 Å. From this cluster model, the following system was created.

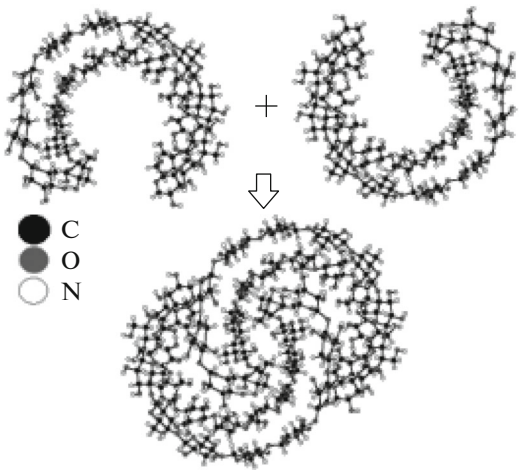

Cellulose II chains containing four atoms of Li in the unit cell (Fig. 7) were deformed by DMAA molecules.

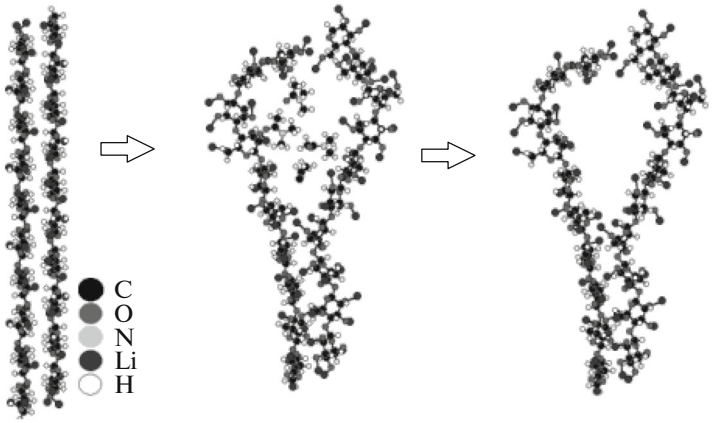

After removal of DMAA molecules, the deformed chains were combined into one cluster. With consideration for the conditions of cellulose regeneration in the DMAA–LiCl system [24], 223 water molecules were added to the final cluster.

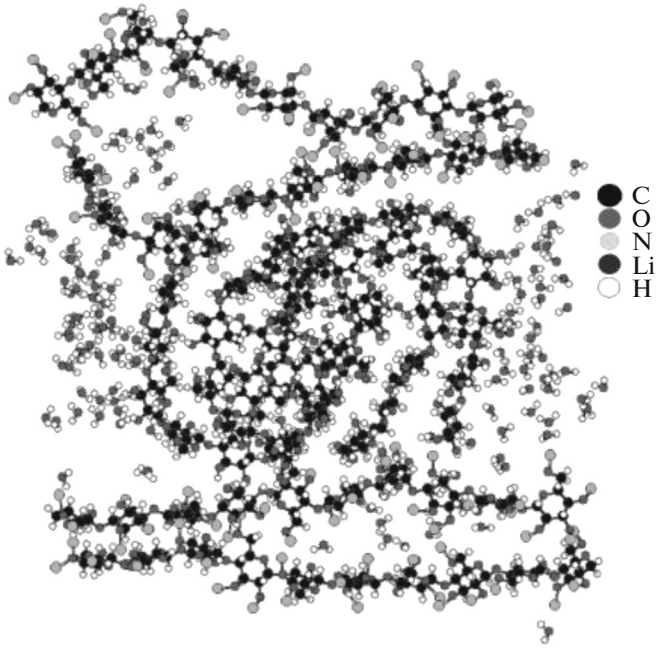

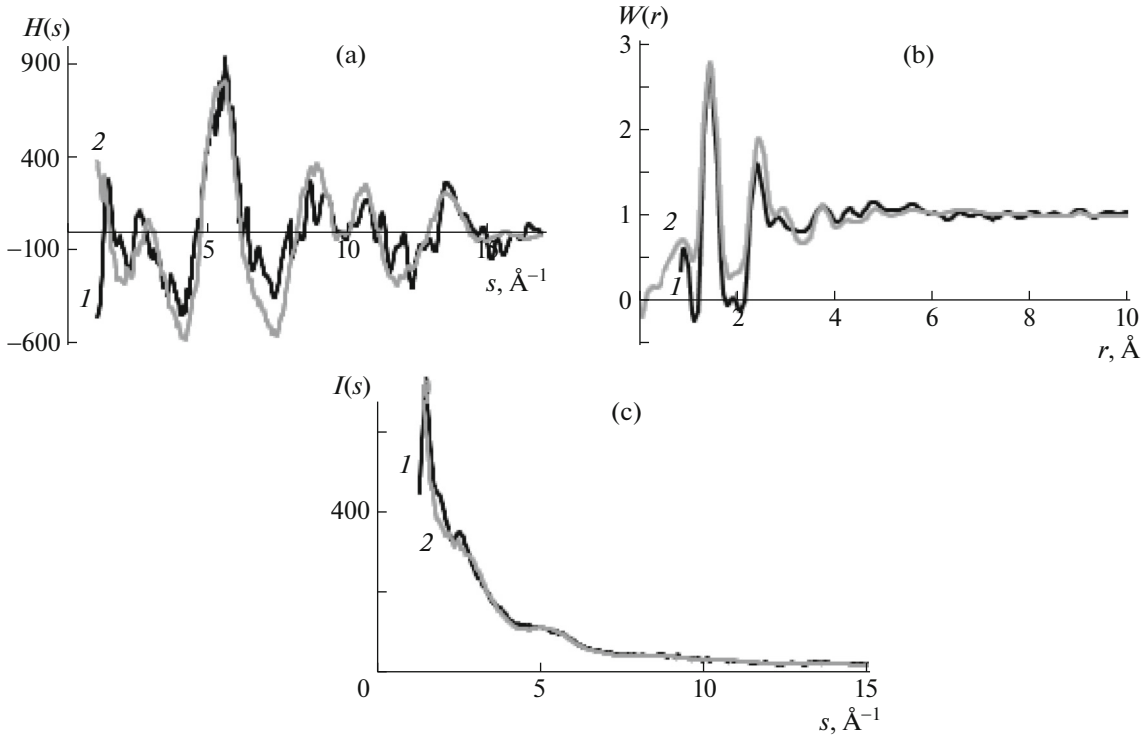

Fig. 11. Distribution curves: (a) interference functions $H(s)$; (b) radial distribution functions of atoms, $W(r)$; and (c) intensities $I(s)$ for (*1*) regenerated cellulose samples in comparison with (*2*) corresponding values for the final cluster model of cellulose.

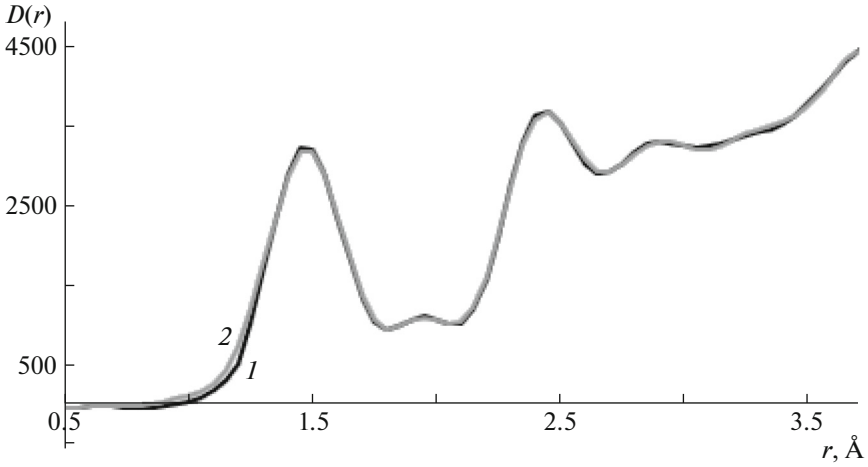

Fig. 12. Distribution curves of pair functions of regenerated sulfate hardwood: (*1*) experimental curve $D(r)$ and (*2*) $D_{LSM}(r)$ calculated with the use of N_{ij} obtained via the least squares method and the values r_{ij} and σ_{ij} found via the trial-and-error search.

Figure 11 shows the $H(s)$, $W(r)$, and $I(s)$ curves for the final cluster. Uncertainty profile factor R_{pm} for the $I(s)$ curves presented in Fig. 11c is 0.08. This value is the lowest for the models used in this study. The maxima on the $H(s)$ and $W(r)$ curves calculated with the use of the model correspond to the values observed on the corresponding experimental curves.

The formula unit of the final cluster is $(C_6O_5H_{8.5}Li_{1.5}) \cdot (H_2O)_{2.8}$. Because the cluster composition differs from the composition of pure cellulose ($C_6O_5H_{10}$), the experimental scattering curve was renormalized to a new composition and the short-range-order characteristics were calculated again (Table 2).

Table 2. Radii r_{ij} and smearing σ_{ij} of coordination spheres and coordination numbers N_{ij} calculated with the use of experimental intensities renormalized to the new composition for regenerated sulfate cellulose in comparison with the corresponding data for cellulose II

Kind of sphere	r_{ij}, Å	r_{ij} (cellulose II), Å	N_{ij}, at.	N_{ij} (cellulose II), at.	σ_{ij}, Å
C–O1	1.46	1.41	1.98	1.0	0.20
C–C1	1.54	1.54	1.62	1.5	0.05
O—Li	1.94	–	0.23	–	0.18
C–O2	2.41	2.41	4.85	3.1	0.15
O–O1	2.85	2.86	4.62	4.6	0.20
O–O2	3.29	3.29	5.91	6.1	0.14
C–O3	3.66	3.66	5.12	3.3	0.10
$\Delta r_{ij} = \pm 0.01$ Å; $\Delta N_{ij} = \pm 0.1$ at.					

Figure 12 presents the experimental $D(r)$ curve and the $D(r)$ curve calculated with the use of the values of r_{ij}, N_{ij}, and σ_{ij} given in Table 2. The degree of discrepancy of the curves is $q = 1\%$.

The values of radii r_{ij} of coordination spheres calculated from the experimental $D(r)$ curves are in agreement with the data for cellulose II, and the values of coordination numbers N_{ij} are higher in almost all the spheres. This circumstance may be explained by the presence of water in the regenerated cellulose. A distance of 1.94 Å corresponds to the sum of ionic radii of lithium and oxygen, while coordination number N_{OLi} corresponds to the quantity of lithium in the model.

CONCLUSIONS

The arrangement of atoms in the short-range-order area in the amorphous cellulose regenerated from the DMAA–LiCl solution is satisfactorily portrayed by the final cluster and comprises, first, two unit cells of cellulose II (four cellulose chains) translated five times among axis *c* and twisted by an angle of 120° and bent by 10 Å; second, two unit cells of cellulose II (four cellulose chains) translated five times among axis *c* with four atoms of Li replacing H atoms in OH bonds in the unit cell that are deformed by DMAA molecules; and, third, 223 water molecules.

The final cluster contains 480 carbon atoms, 623 oxygen atoms, 1126 hydrogen atoms, and 120 lithium atoms. The cluster composition corresponds to the formula unit $(C_6O_5H_{8.5}Li_{1.5}) \cdot (H_2O)_{2.8}$.

The short-range-order characteristics calculated from the experimental distribution curve of pair functions, $D(r)$, show that the lithium ions partially replace hydrogen in OH groups.

REFERENCES

1. C. Olsson and G. Westman, *Cellulose—Fundamental Aspects*, Ed. by T. van de Ven and L. Godbout (In Tech, New York, 2013).
2. G. de Marco Lima, M. R. Sierakowski, P. C. S. Faria-Tischer, and C. A. Tischer, Mater. Sci. Eng. **31** (2), 190.
3. J. He, Z. Liu, H.-Y. Li, G.-H. Wang, and J.-W. Pu, For. Stud. China **9** (3), 217 (2007).
4. C. Zhang, H. Kang, R. Liu, and Y. Huang, J. Phys. Chem. B. **118** (31), 9507 (2014).
5. A. S. Gross, A. T. Bell, and J. W. Chu, J. Phys. Chem. B **117** (12), 3280.
6. K. Mazeau and L. Heux, J. Phys. Chem. B **107** (10), 2394.
7. "Rietveld Method Program, no. 2006610292, March 27, 2006" in *Software Package PDWin 4.0* (Nauchno-proizvodstvennoe predpriyatie "Burevestnik", St. Petersburg, 2004) [in Russian].
8. N. V. Melekh, *Natural and Technical Celluloses. Analysis of Structure* (Izd-vo "LAP", Moscow, 2013) [in Russian].
9. N. V. Melekh, S. V. Frolova and L. A. Aleshina, Polym. Sci., Ser. A **56** (2), 129 (2014).
10. L. A. Aleshina and A. D. Fofanov, *X-ray Structural Analysis of Amorphous Materials* (Izd-vo "PetrGu", Petrozavodsk, 1987) [in Russian].
11. L. A. Aleshina, S. V. Glazkova, M. V. Podoinikova, A. D. Fofanov, and E. V. Silina, Khim. Rastit. Syr'ya, No. **1**, 5 (2001).
12. A. I. Prusskii, L. A. Aleshina, and K. A. Konovalova, *Structure and Physicochemical Properties of Celluloses and Nanocomposites based on Them,* Ed. by L.A. Aleshinoi, V.A. Gurtova, and N.V. Melekh (Izd-vo "PetrGU", Petrozavodsk, 2014), p. 123 [in Russian].
13. G. I. Kobzev, *Application of Nonempirical and Semiempirical Methods in Quantum Chemical Calculations: Manual* (Gos. Orenburgskii Univ., Orenburg, 2004).
14. C. Stan Tsai, *An Introduction to Computational Biochemistry* (Wiley-Liss, New York, 2002).
15. M. E. Solov'ev and M. M. Solov'ev, *Computer Chemistry* (SOLON-Press, Moscow, 2005) [in Russian].
16. L. Norman and J. Allinger, J. Am. Chem. Soc. **99** (25), 8127 (1977).
17. J. T. Sprague, J. C. Tai, Y. Yuh, and N. L. Allinger, J. Comput. Chem. **8**, 581 (1987).
18. N. L. Allinger, R. A. Kok, and M. R. Imam, J. Comput. Chem. **9**, 591 (1988).

19. C. A. Stortz, G. P. Johnson, A. D. French, and G. I. Csonka, Carbohydr. Res. **344**, 2217 (2009).

20. A. G. Gerbst, A. A. Grachev, A. S. Shashkov, and N. E. Nifantiev, Russ. J. Bioorg. Chem. **33** (1), 24 (2007).

21. N. V. Melekh, Candidate's Dissertation in Mathematics and Physics (Petrozavodsk, 2008).

22. A. I. Prusskii, L. A. Aleshina, and K. A. Konovalova, *Structure and Physicochemical Properties of Celluloses and Nanocomposites based on Them,* Ed. by L.A. Aleshinoi, V.A. Gurtova, and N.V. Melekh (Izd-vo "PetrGU", Petrozavodsk, 2014), p. 240 [in Russian].

23. S. J. Hanley, J. F. Revol, L. Godbout, and D. G. Gray, Cellulose **4**, 209 (1997).

24. Yu. V. Bykhovtsova, N. E. Kotel'nikova, and A. M. Mikhailidi, Khim. Rastit. Syr'ya, No. 1 (2014).

Translated by L. Rocha